Journal of Solid State Chemistry **168,** 140–148 (2002)
doi:10.1006/jssc.2002.9701

Synthesis of New Lithium Ionic Conductor Thio-LISICON—Lithium Silicon Sulfides System

Masahiro Murayama,*,† Ryoji Kanno,*,[1] Michihiko Irie,† Shinya Ito,† Takayuki Hata,† Noriyuki Sonoyama,* and Yoji Kawamoto†

*Department of Electronic Chemistry, Interdisciplinary Graduate School of Science and Engineering, Tokyo Institute of Technology, Midori, Yokohama, Kanagawa 226-8502, Japan; and †Department of Chemistry, Faculty of Science, Kobe University, Nada, Kobe, Hyogo 657-8501, Japan

Received February 19, 2002; in revised form May 28, 2002; accepted July 15, 2002

The new lithium ionic conductors, thio-LISICON (LIthium SuperIonic CONductor), were found in the ternary Li_2S–SiS_2–Al_2S_3 and Li_2S–SiS_2–P_2S_5 systems. Their structures of new materials, $Li_{4+x}Si_{1-x}Al_xS_4$ and $Li_{4-x}Si_{1-x}P_xS_4$ were determined by X-ray Rietveld analysis, and the electric and electrochemical properties were studied by electronic conductivity, ac conductivity and cyclic voltammogram measurements. The structure of the host material, Li_4SiS_4 is related to the γ-Li_3PO_4-type structure, and when the Li^+ interstitials or Li^+ vacancies were created by the partial substitutions of Al^{3+} or P^{5+} for Si^{4+}, large increases in conductivity occur. The solid solution member $x=0.6$ in $Li_{4-x}Si_{1-x}P_xS_4$ showed high conductivity of $6.4\times10^{-4}\,S\,cm^{-1}$ at 27°C with negligible electronic conductivity. The new solid solution, $Li_{4-x}Si_{1-x}P_xS_4$, also has high electrochemical stability up to ~5 V vs Li at room temperature. All-solid-state lithium cells were investigated using the $Li_{3.4}Si_{0.4}P_{0.6}S_4$ electrolyte, $LiCoO_2$ cathode and In anode. © 2002 Elsevier Science (USA)

Key Words: **lithium ion conductor; thio-LISICON; lithium silicon sulfide.**

INTRODUCTION

Lithium superionic conductors are of technological importance for future applications as solid electrolytes for all-solid-state lithium batteries and may solve the safety problems of the rechargeable lithium ion batteries using non-aqueous liquid electrolytes (1). Ceramic crystalline electrolytes have advantages over liquid, polymer, gel or even glass electrolytes for their chemical and electrochemical stability. Many attempts to synthesize new ceramic lithium superionic conductors have been made; the highest conductivity of $10^{-3}\,S\,cm^{-1}$ was previously reported for H-doped Li_3N (2). However, the low decomposition potential of ~0.445 V restricts its application as a lithium solid electrolyte (3). In order to improve the stability of the solid electrolytes, a material search is still necessary, and this includes ceramic crystalline materials.

A wide variety of materials have been synthesized in the LISICON [$Li_{14}Zn(GeO_4)_4$] (4) system. The structure is related to the γ-Li_3PO_4 type, and is formed by LiO_4, GeO_4, SiO_4, PO_4, ZnO_4, VO_4 tetrahedra or LiO_6 octahedra. A wide range of solid solutions formed by aliovalent substitutions introduced interstitial lithium ions or lithium vacancies, and led to high ionic conductivities at higher temperatures (5). However, the conductivity values at room temperature (~$10^{-6}\,S\,cm^{-1}$ for $Li_{3.6}Si_{0.6}P_{0.4}O_4$ (6, 7), for example) are still lower than those of copper and silver ionic conductors (8–10).

In order to modify the materials to attain high ionic conductivity, sulfides have a number of advantages over oxides for constructing ionic conductors; i.e., larger ionic radii and more polarizable character of sulfide ions may improve the mobility of the conduction species. Generally speaking, crystalline materials should have higher conductivity than the corresponding glasses, if their crystal structures have been well designed for high ionic conduction. For example, the highest crystalline ionic conductive solids, $Rb_4Cu_{16}I_7Cl_{13}$ (8, 9) and $RbAg_4I_5$ (10), have much higher ionic conductivity than any copper and silver conducting glasses (11). Furthermore, another advantage of crystalline materials is their stability at high temperature. However, inorganic crystalline lithium ion conductors have usually lower conductivities than those of glasses. New material search is still necessary to find high lithium ionic conducting crystalline compounds. Only a few materials have been investigated previously in the crystalline sulfides; Li_3PS_4 (12, 13), Li_4SiS_4 (14) and Li_2SiS_3 (14)

[1] To whom correspondence should be addressed. Fax: +81-45-924-5401. E-mail: kanno@echem.titech.ac.jp.

0022-4596/02 $35.00

were reported to have conductivities of 10^{-7}–10^{-9} S cm^{-1} at room temperature, and no systematic material search has been made.

We found recently the new lithium ionic conductors, thio-LISICON based on the lithium germanium sulfides (15, 16). These compounds have host structures similar to the γ-Li_3PO_4 type, and the conductivities are in the order of 10^{-5}–10^{-3} S cm^{-1} at room temperature. This indicates that there may exist a wide variety of materials in the thio-LISICON system. In the present study, new material search is carried out based on the lithium silicon sulfides, Li_4SiS_4, and new solid solutions were found in the Li_2S–SiS_2–Al_2S_3 and Li_2S-SiS_2–P_2S_5 systems with the family of thio-LISICON.

EXPERIMENTAL

The starting materials were Li_2S, Al_2S_3, and P_2S_5 (Kojundo Chemical Laboratory, >99.9% purity) and SiS_2 (Soekawa Chemicals, >95% purity). These were weighed, mixed in appropriate molar ratios in an argon-filled glove box, put into a carbon-coated quartz tube and heated at a reaction temperature of 700°C for 8 h. After the reaction, the tube was slowly cooled to room temperature.

X-ray diffraction patterns of the powdered samples were obtained with an X-ray diffractometer (Rigaku RU-200B, 12 kW) with Cu$K\alpha$ radiation. The diffraction data were collected at each 0.02° step width over a 2θ range from 20° to 110°. The lattice parameters and structures of the solid solutions, $Li_{4+x}Si_{1-x}Al_xS_4$ and $Li_{4-x}Si_{1-x}P_xS_4$ were refined by X-ray Rietveld analysis using the computer programs, RIETAN-2000 (17).

Ionic conductivity was measured by ac impedance methods in a nitrogen gas flow over a $25°C \le t \le 300°C$ temperature range with an applied frequency range of 10 Hz and 1 MHz using a Solartron 1260 frequency response analyzer. A gold paste used for blocking electrode was painted onto both sides of a sample, and the sample was then heated under vacuum at 150°C for 3 h. Measurements were carried out for the samples with a pellet (8 mm diameter and 2–3 mm thick), and with a rectangular shape ($5 \times 6 \times 2.5$ mm^3) for the solid solutions, $Li_{4+x}Si_{1-x}Al_xS_4$ and $Li_{4-x}Si_{1-x}P_xS_4$, respectively.

Cyclic voltammogram (CV) of the asymmetric Li/$Li_{4-x}Si_{1-x}P_xS_4$ /Au cell was examined using a reference lithium electrode with the scan rate of 1–10 mV s^{-1} and the scan range between –0.2 and 5 V using a Solartron 1287 electrochemical interface.

Electrochemical cells with $LiCoO_2$ and In electrodes were constructed to investigate the cell performances using the new thio-LISICON electrolyte. The electrolyte powder was pressed into a pellet with a diameter of 10 mm and thickness of 1 mm. The positive electrode material is a mixture of $LiCoO_2$ and electrolyte powder in a weight ratio of 1:1. The electrode was pressed together with the electrolyte layer into a two-layered pellet. The charge–discharge curves were measured by constant currents ranging from 10 to 100 μA.

RESULTS AND DISCUSSION

Synthesis and Structures

The Host Material, Li_4SiS_4

In the binary Li_2S–SiS_2 system, two compounds, Li_2SiS_3 and Li_4SiS_4, were reported to exist previously, and their structure models were proposed (14). The X-ray diffraction pattern of Li_4SiS_4 was quite similar to that of Li_4SiO_4 with the γ-Li_3PO_4-type structure; the structure was refined using the structure model of Li_4SiO_4 (18, 19). Table 1 lists the final R factors, lattice and structural parameters with their estimated standard deviations in parentheses. Because of the low scattering factor of Li, the Li positions were not included in the refinements. The results confirmed the γ-Li_3PO_4-type structure similar to that of Li_4GeS_4 (20). Figure 1 shows the structure of Li_4SiS_4. The structure is composed of hexagonal closely packed sulfide ion arrays. The silicon ions are distributed over the tetrahedral sites, and the SiS_4 tetrahedra are isolated from each other. Further study based on neutron diffraction is necessary to clarify the Li positions.

In our material synthesis based on the stoichiometric Li_4SiS_4, solid solutions were examined by aliovalent substitutions, $Si^{4+} \leftrightarrow Li^+ + Al^{3+}$ or $Si^{4+} + Li^+ \leftrightarrow P^{5+}$; this may lead interstitial lithium ions or lithium vacancies according to the formulae, $Li_{4+x}Si_{1-x}Al_xS_4$, and $Li_{4-x}Si_{1-x}P_xS_4$, respectively.

The Ternary Li_2S–SiS_2–P_2S_5 System

The new solid solution was synthesized along the tie line between Li_4SiS_4 and Li_3PS_4 in the ternary Li_2S–SiS_2–P_2S_5 system. The samples synthesized according to the formulae, $Li_{4-x}Si_{1-x}P_xS_4$, showed diffraction patterns similar to the corresponding oxide, Li_4SiO_4. Figure 2 shows the X-ray

TABLE 1
X-Ray Rietveld Refinement Results for Li_4SiS_4

Atom	Site	g	x	y	z	B (Å^2)
Si	2*e*	1	0.6737 (11)	0.25	0.3612 (12)	0.22 (19)
S (1)	4*f*	1	0.8121 (6)	0.0200 (6)	0.2381 (8)	0.63 (15)
S (2)	2*e*	1	0.3657 (9)	0.25	0.2360 (13)	1.3 (2)
S (3)	2*e*	1	0.6757 (10)	0.25	0.7126 (12)	1.3 (2)

Note. $P2_1/m$, $a = 6.8934(3)$ Å, $b = 7.7675(3)$ Å, $c = 6.1241(2)$ Å, $\beta = 91.225(5)°$, $R_{wp} = 11.26\%$, $R_p = 8.72\%$, $R_R = 18.25\%$, $R_e = 5.93\%$, $R_I = 5.97\%$, $R_F = 2.75\%$, $S = R_{wp}/R_e = 1.89$.

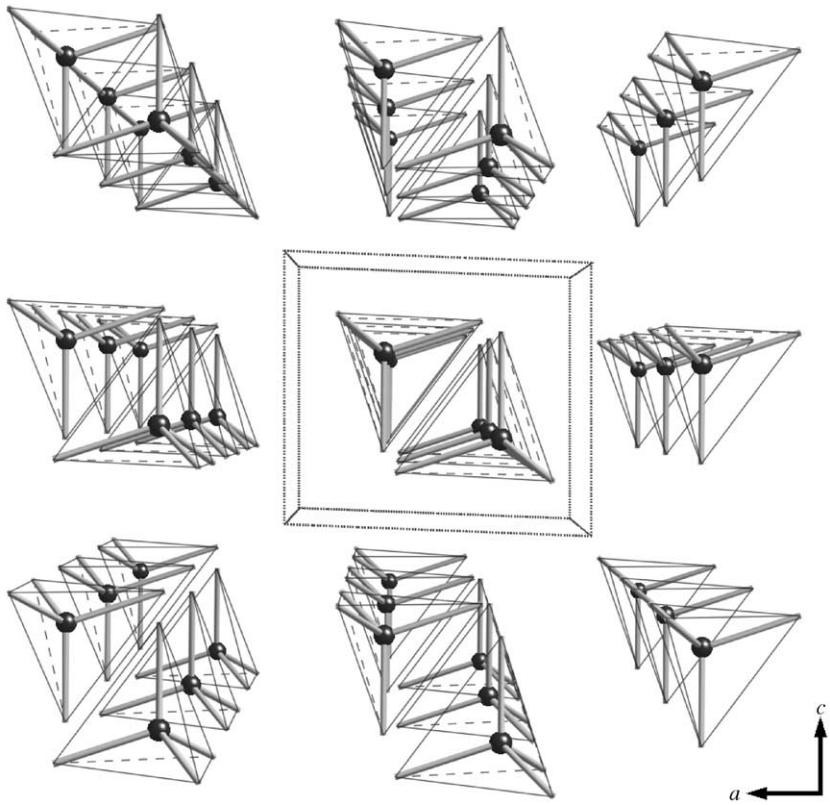

FIG. 1. Structure of Li_4SiS_4. Only SiS_4 tetrahedra is indicated in the figure.

diffraction patterns for the ternary Li_2S–SiS_2–P_2S_5 system. The diffraction patterns showed continuous shift in the diffraction lines from Li_4SiS_4 to Li_3PS_4, which suggests the formation of a solid solution in the whole composition range. A careful analysis of the diffraction data, however, indicated an appearance of superlattice reflections. The patterns in the solid solution were indexed assuming a monoclinic superlattice cell of $2a \times 3b \times 2c$ which is related to the parent lattice ($a \times b \times c$) of the host material, Li_4SiS_4. In the new solid solution, $Li_{4-x}Si_{1-x}P_xS_4$, the $2a \times 3b \times 2c$ superlattice with space group $P2_1/m$ was used for the refinements of the lattice parameters. Figure 3 illustrates the fitted profile and difference patterns for $Li_{4-x}Si_{1-x}P_xS_4$ with $x = 0.8$. Although, the fitting of the pattern is not good enough to solve all the structure parameters, the existence of the superlattice was confirmed. Further studies based on neutron diffraction are necessary.

Figure 4 shows the composition dependence of the lattice parameters in $Li_{4-x}Si_{1-x}P_xS_4$. The lattice parameters plotted in Figure 4 are based on the parent lattice of Li_4SiS_4 with the $a \times b \times c$ cells. Table 2 summarizes the lattice parameter values of $Li_{4-x}Si_{1-x}P_xS_4$. The same type of supperlattice reflections was observed for the solid solution of the thio-LISICON, $Li_{4-x}Ge_{1-x}P_xS_4$ (15). The formation of the superlattice in $Li_{4-x}Ge_{1-x}P_xS_4$ was more complex; the solid solution was divided into three regions; the region I ($0 < x \leq 0.6$) were indexed with a monoclinic superlattice cell of $a \times 3b \times 2c$, the region II ($0.6 < x < 0.8$) with $a \times 3b \times 3c$, and the region III ($0.8 \leq x < 1.0$) with $a \times 2b \times 2c$ cell. These regions of the monoclinic superstructures might correspond to different types of cation ordering. The diffraction data in both systems indicated the formations of the solid solutions in the whole composition range. Neutron diffraction studies are necessary to clarify the structural details on the lithium positions and the origin of the superlattice reflections.

The Ternary Li_2S–SiS_2–Al_2S_3 System

The new solid solution along the tie line between Li_4SiS_4 and Li_5AlS_4 was synthesized in the ternary Li_2S–SiS_2–Al_2S_3 system. The solid solution, $Li_{4+x}Si_{1-x}Al_xS_4$, showed diffraction patterns similar to the corresponding oxide, Li_4SiO_4 with γ–Li_3PO_4-type structure. Figure 5 shows the X-ray diffraction patterns of $Li_{4+x}Si_{1-x}Al_xS_4$. No significant superlattice reflections were observed; the lattice parameters were then refined using the structure of Li_4SiS_4. The lattice parameters changed continuously with

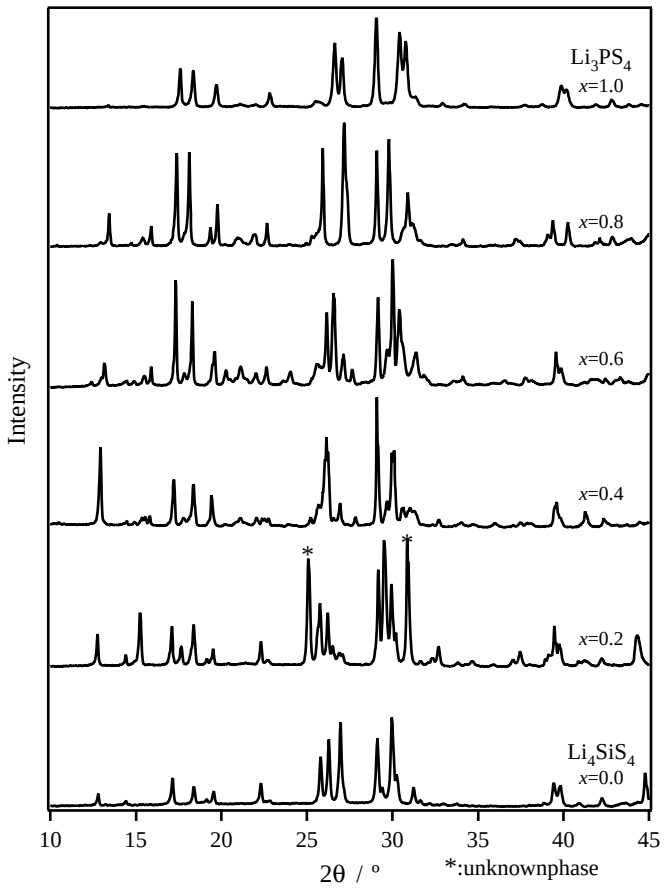

FIG. 2. X-ray diffraction patterns for $Li_{4-x}Si_{1-x}P_xS_4$ in the ternary Li_2S–SiS_2–P_2S_5 system.

x in $Li_{4+x}Si_{1-x}Al_xS_4$ as shown in Fig. 6, which indicates the formation of a whole range of solid solution, $0.0 \le x \le 1.0$.

Electrical Properties

The Ternary Li_2S–SiS_2–P_2S_5 System

Ionic conductivity was measured with an ac impedance method over a $25^\circ C \le t \le 300^\circ C$ temperature range with an applied frequency range of 10 Hz–1 MHz.The conductivity values were determined from the impedance plots of the data. Figures 7(a) and 7(b) show the impedance plots of $Li_{4-x}Si_{1-x}P_xS_4$ with $x = 0.4$ and 0.6, respectively. A semicircle was observed for the sample, $x = 0.4$, at 25°C in the high-frequency range with a spike in the low-frequency range which is caused by an electrode contribution (Fig. 7(a)). The semicircle was interpreted as a parallel combination of a resistance and a capacitance, and is attributed to the bulk and grain boundary contribution, which was estimated by those capacitance values of 10^{-9}–10^{-10} F, and the spike to the electrode contribution. However, the bulk and grain boundary contributions could not be separated. At high temperature, no semicircle was observed and only a spike caused by the electrode contribution was observed. For the sample, $x = 0.6$ in $Li_{4-x}Si_{1-x}P_xS_4$, only a spike caused by an electrode contribution was observed even at 27°C (Fig. 7(b)). The behavior of the impedance plots shows the characteristics of a pure ionic conductor composed of bulk and electrode contributions where the bulk resistance values were calculated from the intercept of the spike. No differences in conductivities were observed between the cooling and heating process during the measurements.

The temperature dependences of the conductivities in $Li_{4-x}Si_{1-x}P_xS_4$ are shown in Fig. 8. Plotted against the compositions in Fig. 9 are the conductivities and the activation energies. The conductivity continuously increased as the P content increased from $x = 0.0$ to 0.6 in $Li_{4-x}Si_{1-x}P_xS_4$, and the highest conductivity value of

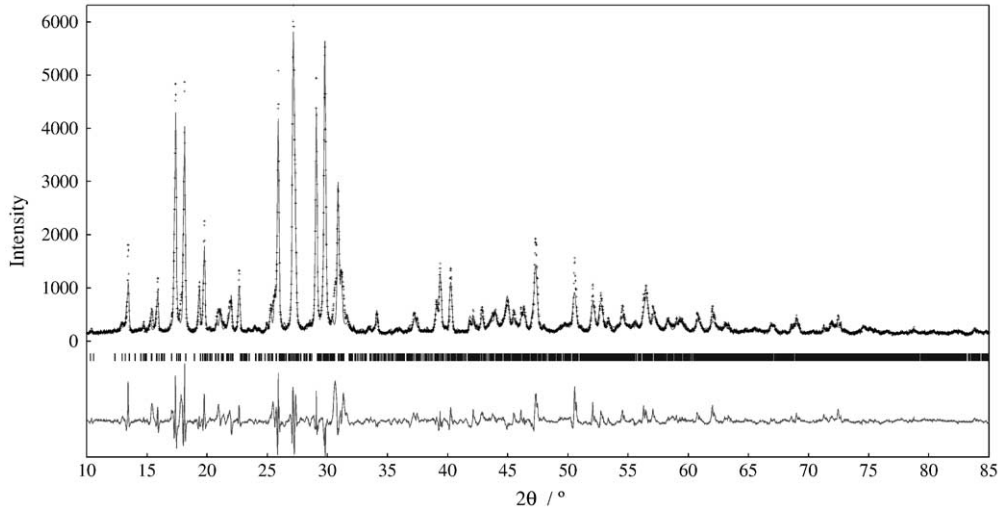

FIG. 3. X-ray Rietveld refinement pattern for $Li_{3.2}Si_{0.2}P_{0.8}S_4$.

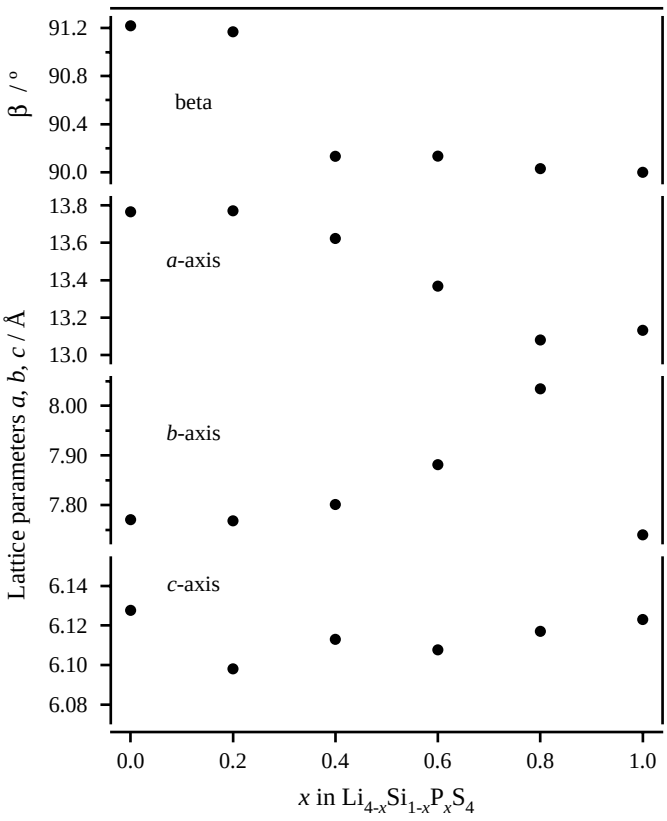

FIG. 4. Composition dependence of the lattice parameters in $Li_{4-x}Si_{1-x}P_xS_4$ determined by XRD measurements. The lattice parameters plotted in the figure are based on the parent lattice of the LISICON with the $a \times b \times c$ cells.

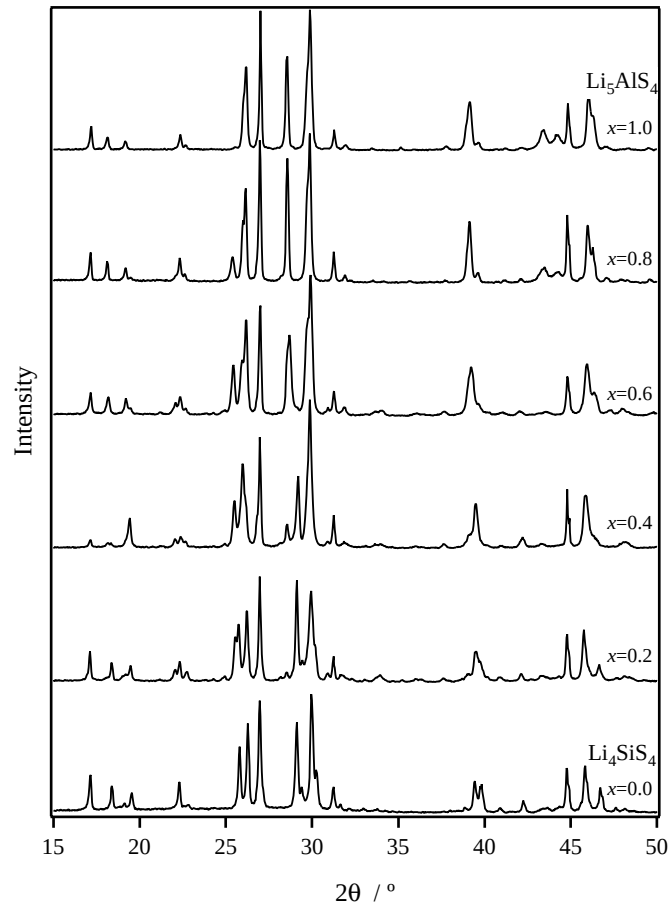

FIG. 5. X-ray diffraction patterns for $Li_{4+x}Si_{1-x}Al_xS_4$ in the ternary Li_2S–SiS_2–Al_2S_3 system.

$6.4 \times 10^{-4}\,S\,cm^{-1}$ at 27°C was obtained. At the same time, the activation energy decreased with x to the lowest value of 27.6 kJ mol^{-1} (0.29 eV) at $x = 0.6$.

The Ternary Li_2S–SiS_2–Al_2S_3 System

Figure 10 shows the impedance plots for $Li_{4.8}Si_{0.2}Al_{0.8}S_4$. A semicircle observed at 90°C, 130°C, and 150°C is composed of the bulk and grain boundary, and each contribution could not be separated. The resistivity values were therefore calculated by the intercept of the semicircle.

TABLE 2
Lattice Parameters in $Li_{4-x}Si_{1-x}P_xS_4$

x	a (Å)	b (Å)	c (Å)	β (deg)
0.0	6.8825 (5)	7.7710 (6)	6.1276 (5)	91.215 (8)
0.2	13.7707 (12)	23.304 (2)	12.1962 (8)	91.168 (8)
0.4	13.6233 (11)	23.4044 (19)	12.2258 (7)	90.133 (14)
0.6	13.3678 (9)	23.6448 (18)	12.2154 (7)	90.134 (11)
0.8	13.0804 (7)	24.1028 (14)	12.2338 (5)	90.030 (8)
1.0	13.1320 (11)	7.7402 (7)	6.1230 (4)	90.000

Figure 11(a) shows the temperature dependences of the conductivities in $Li_{4+x}Si_{1-x}Al_xS_4$. The composition dependences of the conductivities and the activation energies at room temperature are also shown in Fig. 11(b). The highest conductivity and the lowest activation energy were obtained at the composition $x = 0.8$ in $Li_{4+x}Si_{1-x}Al_xS_4$ with the conductivity and activation energy values of $2.3 \times 10^{-7}\,S\,cm^{-1}$ and 50.3 kJ mol^{-1}, respectively. The conductivity values of the thio-LISICON with the silicon system are comparable for the germanium system ($6.5 \times 10^{-5}\,S\,cm^{-1}$) for $Li_{4.275}Ge_{0.61}Ga_{0.25}S_4$ (16).

Comparison with Other Ionic Conductors

In aliovalent solid solution, ions are substituted by other ions of different charge, which causes consequently additional changes involving creation of vacancies or interstitials (ionic compensation), or electrons or holes (electronic compensation) to preserve electroneutrality. It is reasonable to assume the former mechanism because no transition elements exist as a constituent of the thio-LISICON, which likely forms pure ionic conduction as a

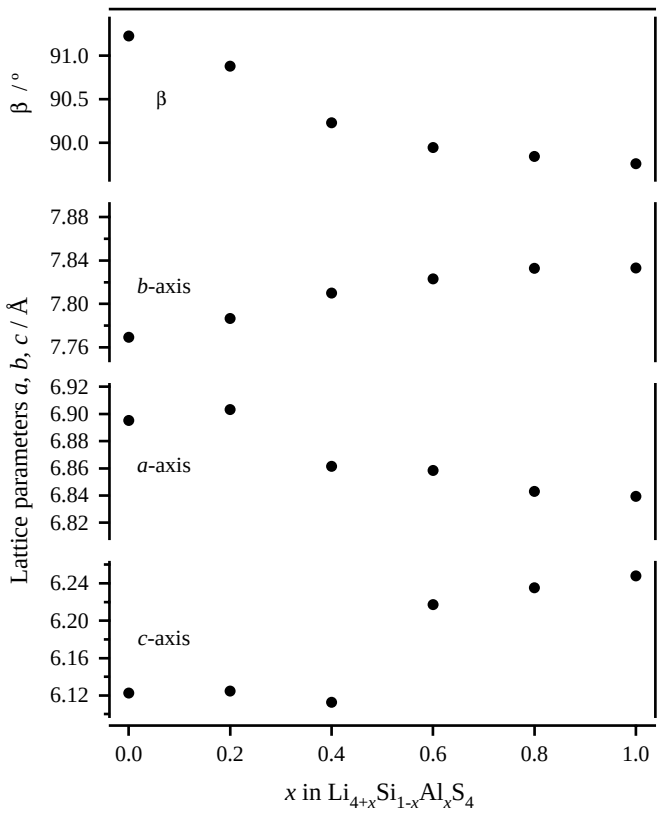

FIG. 6. Lattice parameter changes in $Li_{4+x}Si_{1-x}Al_xS_4$.

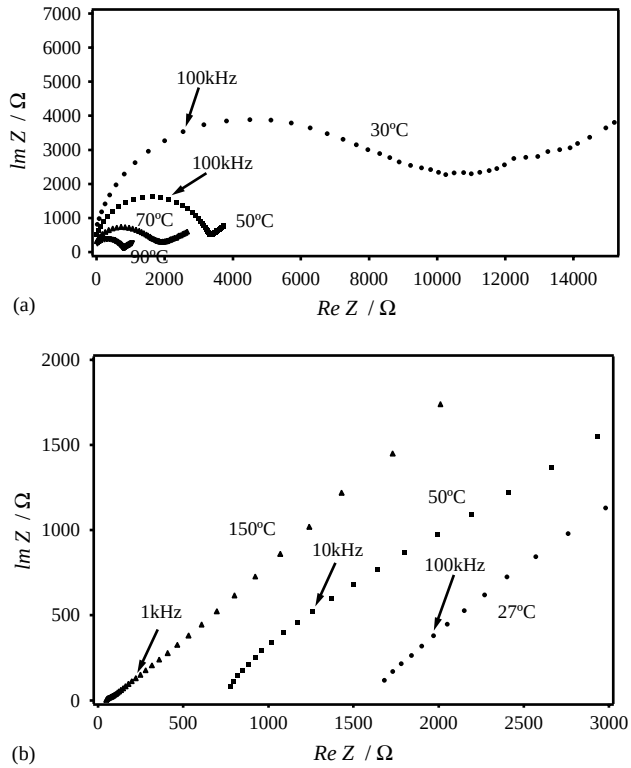

FIG. 7. Complex impedance plots for $Li_{4-x}Si_{1-x}P_xS_4$ at $x=0.4$ (a) and $x=0.6$ (b).

result. The partial substitution of P^{5+} for Si^{4+} may introduce lithium vacancy, and increase the conductivity. The conductivity value of the new thio-LISICON ($6.4\times10^{-4}\,S\,cm^{-1}$ at 27°C) is much higher than those of the oxide LISICON, $Li_{14}Zn(GeO_4)_4$ (4) and $Li_{3.6}Si_{0.6}P_{0.4}O_4$ (6, 7) by two or three orders of magnitude. The conductivity-value is also comparable to those of the previous ceramic lithium superionic conductors, the intrinsic Li_3N ($2–4\times10^{-4}\,S\,cm^{-1}$) (2), H-doped Li_3N ($6\times10^{-3}\,S\,cm^{-1}$) (2) and $La_{0.62}Li_{0.16}TiO_3$ ($1\times10^{-4}\,S\,cm^{-1}$) (21), and the modified sulfide glasses, $Li_2S–SiS_2–LiI$ ($1.8\times10^{-3}\,S\,cm^{-1}$) (22) and $Li_2S–SiS_2–Li_3PO_4$ ($6.9\times10^{-4}\,S\,cm^{-1}$) (23). Among the thio-LISICON compounds, the conductivity-value of the new solid solution, $Li_{4-x}Si_{1-x}P_xS_4$ is of one order magnitude lower than that of $Li_{4-x}Ge_{1-x}P_xS_4$, which showed the highest conductivity of $2.2\times10^{-3}\,S\,cm^{-1}$ at room temperature (15).

Electrochemical Properties

The electrochemical stability was examined by the CV of the $Li/Li_{3.4}Si_{0.4}P_{0.6}S_4/Au$ cell using a reference lithium electrode. Figures 12(a) and 12(b) show the CV of the asymmetric cell. In the scan range between 2 and 5 V vs Li, no significant currents corresponding to the electrolyte

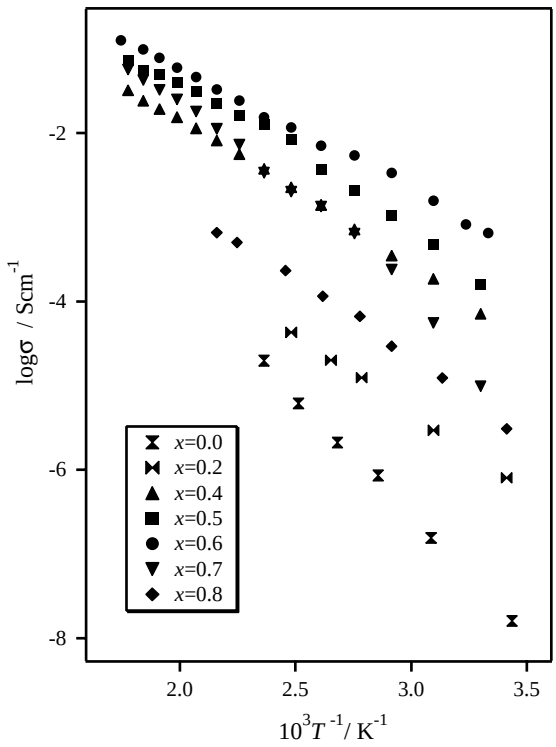

FIG. 8. Temperature dependences of the conductivities for $Li_{4-x}Si_{1-x}P_xS_4$ synthesized at 700°C.

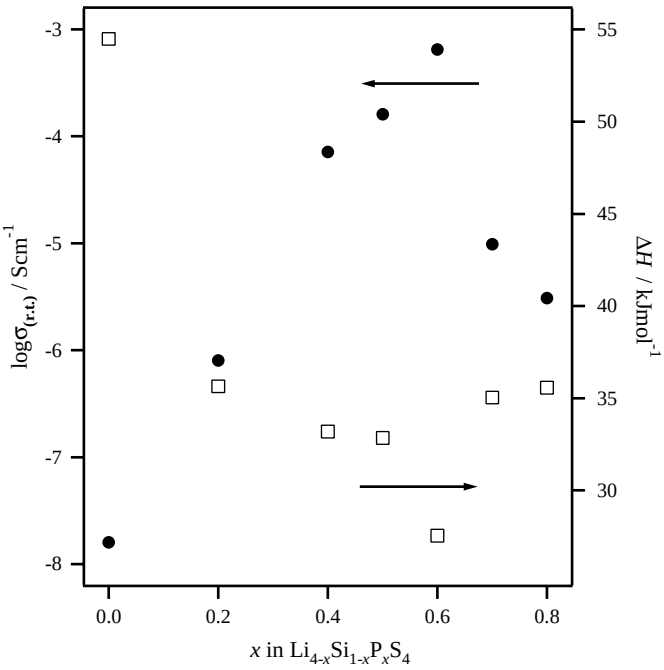

FIG. 9. Composition dependence of the conductivities and the activation energies for $Li_{4-x}Si_{1-x}P_xS_4$.

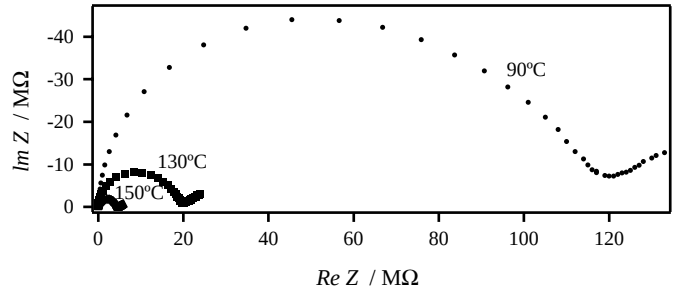

FIG. 10. Complex impedance plots for $Li_{4.8}Si_{0.2}Al_{0.8}S_4$.

decomposition were observed (Fig. 12(a)). In the scan range between −0.2 and 5 V, only cathodic and anodic currents were observed near 0 V vs Li corresponding to the lithium deposition reaction ($Li^+ + e^- \rightarrow Li$) and the dissolution reaction ($Li \rightarrow Li^+ + e^-$), respectively (Fig. 12(b)). Since no significant decomposition current was observed, the new thio-LISICON was stable up to 5 V. The CV behavior observed for $Li_{3.4}Si_{0.4}P_{0.6}S_4$ was similar to those of the solid solution, $Li_{4-x}Ge_{1-x}P_xS_4$ (15) and the Li_2S–SiS_2–Li_3PO_4 glasses (23). Following these measurements, the surface of the electrolyte which was attached to the lithium metal was characterized by X-ray diffraction measurements. No significant changes in the diffraction pattern were observed; $Li_{3.4}Si_{0.4}P_{0.6}S_4$ was stable in contact with lithium metal.

The In/$LiCoO_2$ electrochemical cells were constructed to investigate the cell performances using the new thio-LISICON electrolyte. The electrolyte powder was pressed

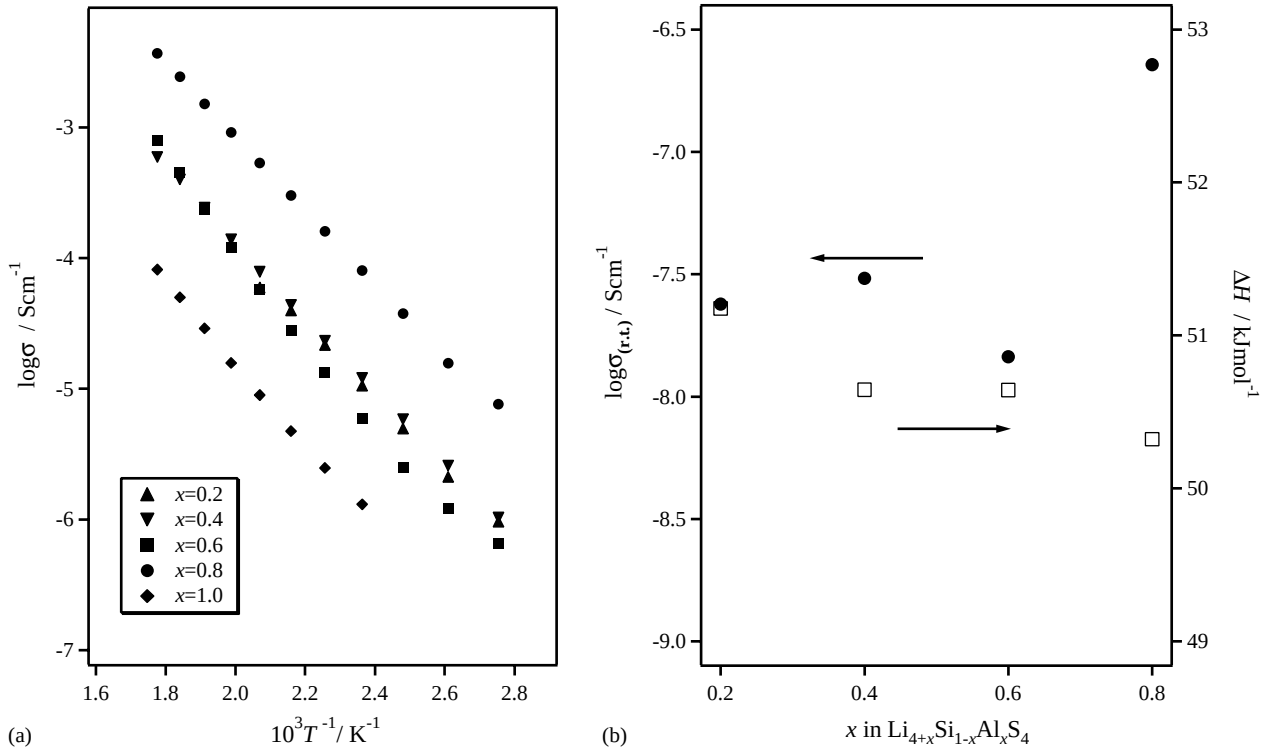

FIG. 11. Temperature dependences of the conductivities for $Li_{4+x}Si_{1-x}Al_xS_4$ synthesized at 700°C (a). Composition dependence of the conductivities and the activation energies for $Li_{4+x}Si_{1-x}Al_xS_4$ (b).

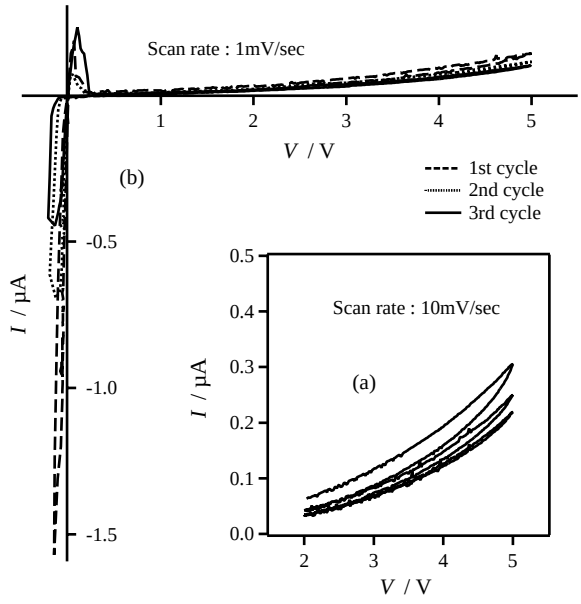

FIG. 12. CV of the cell, Li/ $Li_{3.6}Si_{0.4}P_{0.6}S_4$/Au, using reference Li electrode. The scan rate was 10 mV s^{-1}, and the scan ranges were 2–5 V vs Li^+/Li (a). The scan rate was 1mV s^{-1}, and the scan ranges were –0.2–5 V vs Li^+/Li (b).

into a pellet with a diameter of 10 mm and thickness of 1 mm. The positive electrode material is a mixture of $LiCoO_2$, the electrolyte powder, and acetylene black in a weight ratio of 5:5:1. It was pressed together with the electrolyte layer into a two-layered pellet at a pressure of 5900 kg cm^{-2}. A piece of indium foil was attached to the face of the electrolyte layer as a negative electrode. Figure 13 shows the results on the charge and discharge experiments. The cells were charged and discharged from 1.0 to 4.5 V at constant current densities of 13–127 μA cm^{-2} at room temperature. At a current density of 13 μA cm^{-2}, the charge–discharge capacity was 120 mA h g^{-1} without any significant overpotential of the cell. However, the large difference in voltage between the charge and discharge process for a current density of 127 μA cm^{-2} indicated a large overpotential of the cell. The In/$LiCoO_2$ electrochemical cell using $Li_{4-x}Si_{1-x}P_xS_4$ electrolyte has higher capacity and can be operated at higher current density than the cell using $Li_{4+x+\delta}(Ge_{1-\delta'-x}Ga_x)S_4$ electrolyte (16).

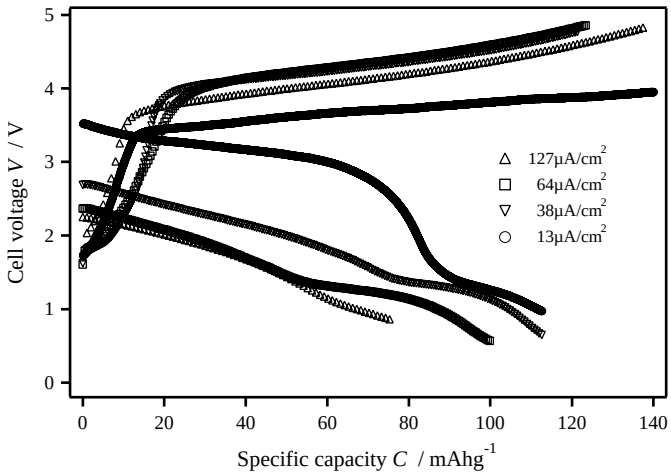

FIG. 13. Charge–discharge curves of In/$LiCoO_2$ cell. The current densities were 13–127 μA cm^{-2}.

CONCLUSION

The new thio-LISICON compounds based on lithium silicon sulfides were found to exist and to have a high ionic conductivity of 6.4×10^{-4} S cm^{-1} at room temperature for $Li_{3.4}Si_{0.4}P_{0.6}S_4$. The material shows high electrochemical stability and no reaction with lithium metal. Based on the stoichiometric Li_4SiS_4, lithium vacancies and interstitial lithium ions were introduced by aliovalent substitutions of $Si^{4+} \Leftrightarrow Li^+ + Al^{3+}$ and $Si^{4+} + Li^+ \Leftrightarrow P^{5+}$, respectively. The conductivity increased in both substitutions. An all-solid-state lithium cell using In/$Li_{3.4}Si_{0.4}P_{0.6}S_4$/$LiCoO_2$ was operated at high voltage (4.5 V). The cell was charged and discharged at currents of > 127 μA cm^{-2}.

ACKNOWLEDGMENTS

This work was supported partly by the Grant-in-Aid for Scientific Research from The Ministry of Education, Science, Sports and Culture of Japan, and by a grant from Genesis Research Institute.

REFERENCES

1. S. Kondo, *in* "Lithium Ion Batteries" (M. Wakihara, O. Yamamoto, Eds.), Chap. 9. Kodansha, Tokyo, 1998.
2. T. Lapp, S. Skaarup, and A. Hooper, *Solid State Ionics* **11,** 97 (1983).
3. A. Rabenau, *Solid State Ionics* **6,** 277 (1982).
4. H. Y.-P. Hong, *Mat. Res. Bull.* **13,** 117 (1978).
5. A. R. West, *in* "Solid State Electrochemistry" (P. G. Bruce, Ed.), Chap. 2. Cambridge University Press, Cambridge, UK, 1995.
6. Y.-W. Hu, I. D. Raistrick, and R. A. Huggins, *J. Electrochem. Soc.* **124,** 1240 (1977).
7. R. D. Shannon, B. E. Taylor, A. D. English, and T. Berzins, *Electrochim. Acta* **22,** 783 (1977).
8. T. Takahashi, O. Yamamoto, S. Yamada, and S. Hayashi, *J. Electrochem. Soc.* **126,** 1654 (1979).
9. R. Kanno, K. Ohno, Y. Kawamoto, Y. Takeda, O. Yamamoto, T. Kamiyama, H. Asano, F. Izumi, and S. Kondo, *J. Solid State Chem.* **102,** 79 (1993).
10. B. B. Owens and G. R. Argue, *J. Electrochem. Soc.* **117,** 898 (1970).
11. J. Kuwano and M. Kato, *Denki Kagaku* **46,** 353 (1978).
12. M. Tachez, J.-P. Malugani, R. Mercier, and G. Robert, *Solid State Ionics* **14,** 181 (1984).
13. R. Mercier, J.-P. Malugani, B. Fahys, and G. Robert, *Acta Crystallogr. Struct. Crystallogr. Cryst. Chem.* **38,** 1887 (1982).
14. B. T. Ahn and R. A. Huggins, *Mater. Res. Bull.* **24,** 889 (1989).

15. R. Kanno and M. Murayama, *J. Electrochem. Soc.* **148,** 742 (2001).
16. R. Kanno, T. Hata, Y. Kawamoto, and M. Irie, *Solid State Ionics* **130,** 97 (2000).
17. F. Izumi and T. Ikeda, *Mater. Sci. Forum* **321–324,** 198 (2000).
18. W. H. Baur and T. Ohta, *J. Solid State Chem.* **44,** 50 (1982).
19. V. W. Gratzer, H. Bittner, H. Nowotny, and K. Seifert, *Z. Kristallogr., Kristallophys., Kristallochem.* **133,** 260 (1971).
20. M. Murayama, R. Kanno, Y. Kawamoto, and T. Kamiyama, *Solid State Ionics*, in press.
21. Y. Inaguma, L. Chen, M. Itou, and T. Nakamura, *Solid State Ionics* **70/71,** 196 (1994).
22. J. H. Kennedy and Y. Yang, *J. Solid State Chem.* **69,** 252 (1987).
23. S. Kondo, K. Takada, and Y. Yamamura, *Solid State Ionics* **53–56,** 1183 (1992).